MedChemComm

RESEARCH ARTICLE

View Article Online
View Journal | View Issue

Cite this: *Med. Chem. Commun.*, 2018, **9**, 632

Anti-cancer effect of a novel 2,3-didithiocarbamate-substituted naphthoquinone as a tumor metabolic suppressor *in vitro* and *in vivo*†

Xianling Ning,[a] Yunqiao Li,[ac] Hailong Qi,[ab] Ridong Li,[a] Yan Jin,[a] Junyi Liu*[d] and Yuxin Yin*[abc]

Received 2nd February 2018,
Accepted 20th February 2018

DOI: 10.1039/c8md00062j

rsc.li/medchemcomm

Tumor cells reprogram their cellular metabolism by switching from oxidative phosphorylation to aerobic glycolysis to support aberrant cell proliferation. Suppressing tumor cell metabolism has become an attractive strategy for treating cancer patients. In this study, we identified a 2,3-didithiocarbamate-substituted naphthoquinone **3i** that inhibited the proliferation of tumor cells by disturbing their metabolism. Compound **3i** reduced cancer cell viability with IC_{50} values from 50 nM to 150 nM against HCT116, MCF7, MDA-MB231, HeLa, H1299 and B16 cells. Further, compound **3i** was found to suppress ATP production in cultured cancer cells, inhibit the M2 isoform of pyruvate kinase (PKM2) which is a rate-limiting enzyme in the glycolytic pathway and block the subsequent transcription of the downstream genes GLUT1, LDH and CCND1. In addition, exposure to compound **3i** significantly suppressed tumor growth in a B16 melanoma transplantation mouse model and a spontaneous breast carcinoma mouse model *in vivo*. The identification of compound **3i** as a tumor metabolic suppressor not only offers a candidate compound for cancer therapy, but also provides a tool for an in-depth study of tumor metabolism.

1. Introduction

Cancer cells differ from most normal cells in metabolism. Normal cells rely generally on mitochondrial oxidative phosphorylation to generate energy from glucose, whereas cancer cells instead rely on glycolysis.[1–4] This difference suggests that targeting tumor metabolism could be a selective approach to suppress tumor growth.[5–7] Glucose goes through a series of biochemical transformations with production of ATP in the process of glycolysis, and each step is catalyzed by specific enzymes.[5] Influencing these enzymes to reduce or reverse the abnormal reprogrammed metabolism of cancer cells is an attractive therapeutic strategy for cancer patients. Pyruvate kinase (PK) is a rate-limiting enzyme that regulates the final step in glycolysis and catalyzes the transfer of a phosphate group from phosphoenolpyruvate (PEP) to adenosine diphosphate (ADP) to yield pyruvate and adenosine triphosphate (ATP).[8,9] There are four isoforms of PK (M1, M2, L and R) in mammalian cells: the M1 isoform (PKM1) is expressed in many differentiated tissues, PKM2 is expressed during embryonic development and overexpressed in tumor tissues, PKL and PKR are expressed in liver and erythrocytes, respectively.[10–12] Many studies have shown that tumorigenesis is connected with the re-expression of PKM2 together with downregulation of the expression of PKM1 and other isozymes.[9,13] In addition, PKM2 activates β-catenin to induce CCDN1 and c-Myc expression and upregulate GLUT1 and lactate dehydrogenase A (LDHA).[14–17] Upregulation of these glycolysis genes increases glucose intake, consumption and lactate production to promote tumorigenesis.[1]

We previously synthesized a series of dithiocarbamate-substituted naphthoquinone derivatives and evaluated their anti-proliferative effects at the cellular level and PKM2 inhibition activity at the enzyme level.[18,19] To further improve the activity, we continue to optimize the structure. In this study, we synthesized a new 2,3-didithiocarbamate-substituted naphthoquinone compound **3i** (Fig. 1A), which exhibited a more potent anti-proliferative effect than previously synthesized compounds. It reduced cancer cell viability with IC_{50} values from 50 nM to 100 nM against HCT116, MCF7, MDA-MB231, HeLa, H1299 and B16 cells. We also found that compound **3i** suppressed tumor cell metabolism by reducing ATP

[a] *Institute of Systems Biomedicine, School of Basic Medical Sciences, Beijing Key Laboratory of Tumor Systems Biology, Peking University Health Science Center, Beijing, China. E-mail: yinyuxin@hsc.pku.edu.cn*
[b] *Peking-Tsinghua Center for Life Sciences, Peking University Health Science Center, Beijing, China*
[c] *Department of Pathology, School of Basic Medical Sciences, Peking University Health Science Center, Beijing, China*
[d] *State Key Laboratory of Natural and Biomimetic Drugs, Department of Chemical Biology, School of Pharmaceutical Sciences, Peking University Health Science Center, Beijing, China. E-mail: jyliu@bjmu.edu.cn*

† Electronic supplementary information (ESI) available. See DOI: 10.1039/c8md00062j

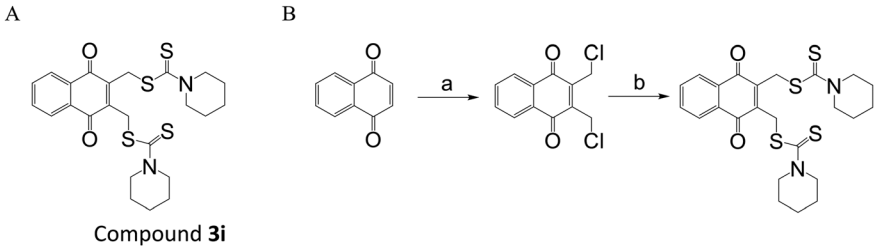

Fig. 1 The structure of and synthetic route toward compound **3i**. (A) The structure of compound **3i**. (B) The synthetic route toward compound **3i**. Reagents and conditions: (a) formaldehyde, HCl, HAc, H_2O, 0 °C, 68.9%; (b) CS_2, piperidine, CH_3CN, rt, 83.5%.

production in cancer cells, inhibiting PKM2 activity and blocking the subsequent transcription of the downstream genes GLUT1, LDH and CCND1. In addition, exposure to compound **3i** significantly suppressed tumor growth in a B16 melanoma transplantation mouse model and a spontaneous breast carcinoma mouse model *in vivo*.

2. Materials and methods

2.1 Synthesis of compound 3i

2.1.1 Procedure for preparation of 2,3-bis-chloromethyl-[1,4]naphthoquinone. The 1,4-naphthoquinone (1 g, 6.3 mmol) in glacial acetic acid (20 mL) was placed in a 100 mL round-bottomed flask, and 36% aqueous formaldehyde (6 mL) was added. The reaction solution was cooled in ice-water. Dry hydrogen chloride was passed in for 2 h. The solution became red, then was kept at room temperature for 48 h. The reaction mixture was poured onto ice and extracted with ethyl acetate. The combined organic fractions were washed with brine, dried (Na_2SO_4), and concentrated under reduced pressure. Purification of the crude residue by column chromatography (petroleum ether/ethyl acetate) afforded the title compound (yellow solid). The yield of this reaction was 68.9%. ^{1}H NMR (400 MHz, $CDCl_3$) δ 8.18–8.20 (m, 2H, Ar*H*), 7.81–7.83 (m, 2H, Ar*H*), 4.72 (s, 4H, 2CH_2Cl).

2.1.2 Procedure for preparation of dipiperidine-dithiocarbamic acid 3-dipiperidinethiocarbamoylsulfanylmethyl-1,4-dioxo-1,4-dihydronaphthalen-2-ylmethyl ester (3i). Carbon disulfide (180 μL, 3 mmol) and piperidine (297 μL, 3 mmol) were added to CH_3CN (5 mL) and the resulting solution was stirred for 30 minutes. 2,3-Bis-chloromethyl-[1,4]naphthoquinone (254 mg, 1 mmol) was added in portions at frequent intervals. Then, the reaction mixture was kept at room temperature for 48 h. The reaction mixture was concentrated *in vacuo*, diluted with H_2O, and extracted with CH_2Cl_2. The combined organic fractions were washed with brine, dried (Na_2SO_4), and concentrated under reduced pressure. Purification of the crude residue by column chromatography (petroleum ether/CH_2Cl_2) afforded compound **3i** (yellow solid). The yield of this reaction was 83.5%. Mp 142–143 °C. ^{1}H NMR (400 MHz, $CDCl_3$) δ 8.11–8.13 (m, 2H, Ar*H*), 7.73–7.75 (m, 2H, Ar*H*), 4.86 (s, 4H, 2CH_2S), 4.29 (q, 4H, 2NCH_2), 3.87 (q, 4H, 2NCH_2), 1.70 (m, 12H, 2$CH_2CH_2CH_2$). ^{13}C NMR (100 MHz, $CDCl_3$) δ 194.21, 183.95, 143.97, 133.84, 132.05, 126.65, 34.11, 24.25. HR-MS (ESI$^+$) *m/z*: 505.1112 $[M + H]^+$, 527.0931 $[M + Na]^+$. Found: 505.1100 $[M + H]^+$, 527.0903 $[M + Na]^+$.

Table 1 *In vitro* cytotoxicity of compound **3i**

	IC_{50} ± SD (μM)
HCT116	0.077 ± 0.011
MCF7	0.061 ± 0.030
MDA-MB231	0.135 ± 0.010
HeLa	0.124 ± 0.010
H1299	0.109 ± 0.015
B16	0.104 ± 0.007
BEAS-2B	32.61 ± 2.04

2.2 Cell culture

Cell lines were grown with routine culture techniques in RPMI 1640 supplemented with 9% fetal bovine serum at 37 °C in 5% CO_2.

2.3 MTS cell proliferation assay

Cells were plated in 96-well plates at a density of 5000–10 000 cells per well. 12 h after seeding, the cells were treated with

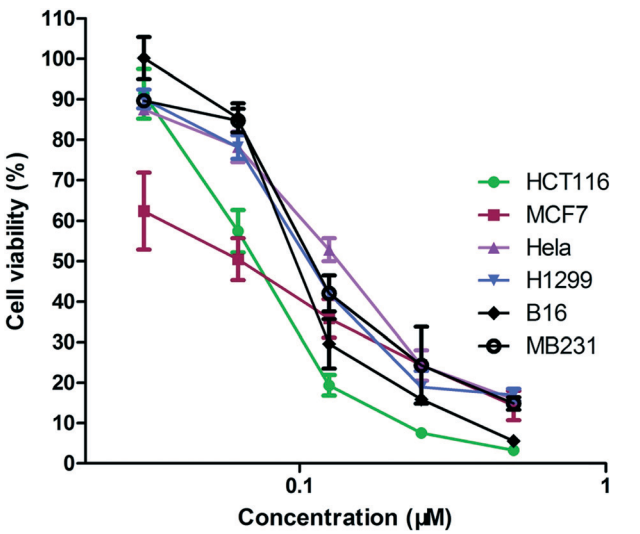

Fig. 2 Compound **3i** reduces cancer cell viability. Cells were treated with increasing concentrations of compound **3i**. Cell viability was measured using MTS.

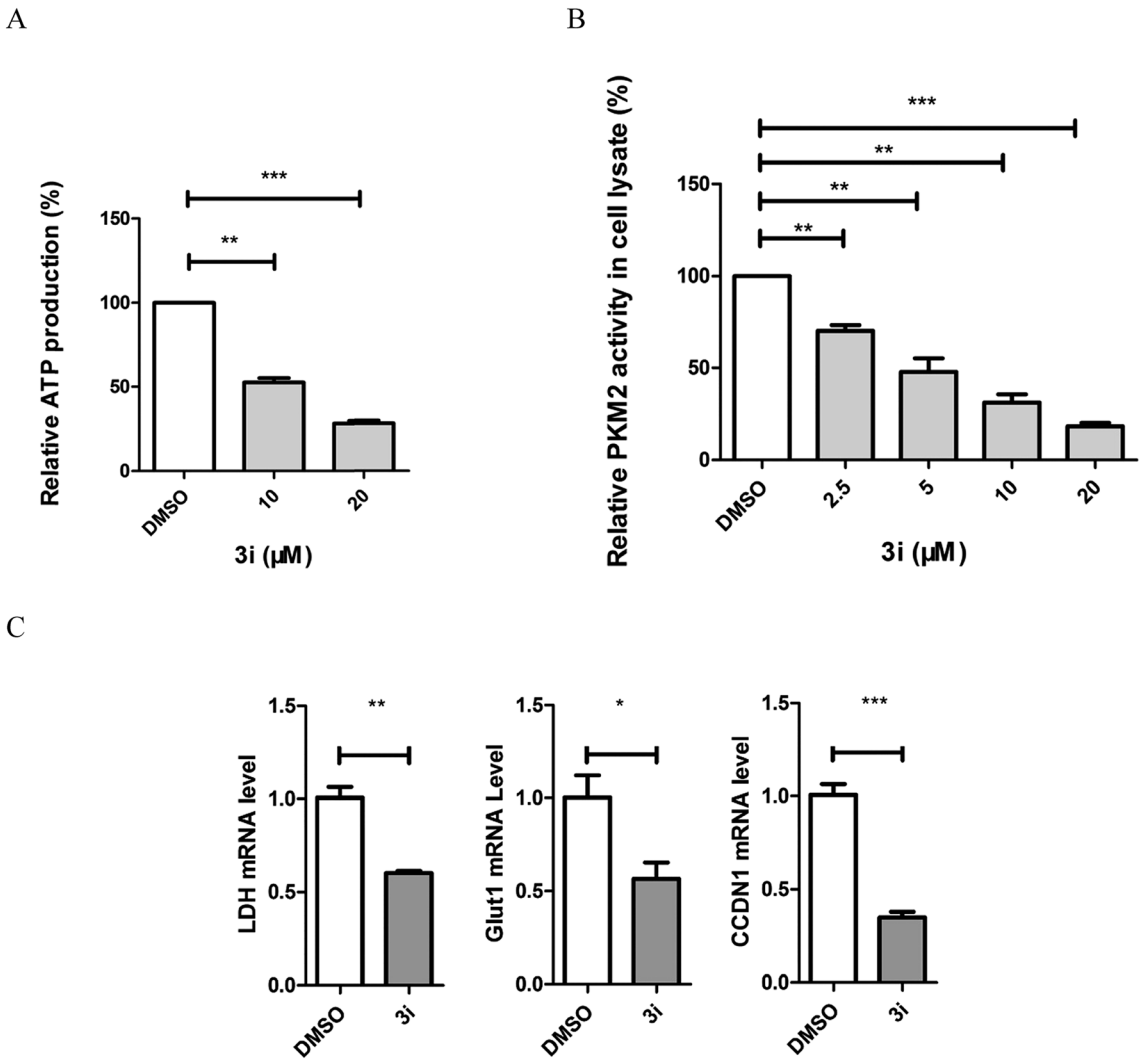

Fig. 3 Compound **3i** can regulate the metabolism of tumor cells. (A) Compound **3i** inhibited cellular ATP production. HCT116 cells were treated with 10 μM and 20 μM compound **3i** for 6 h and ATP production was tested with an ATP assay kit. (B) Compound **3i** inhibited PKM2 activity in cells in a dose-dependent manner. HCT116 cells were treated with 2.5 μM, 5 μM, 10 μM and 20 μM compound **3i** for 8 h and PKM2 activity was tested in the corresponding cell lysates using a fluorescence PK–LDH coupled assay. (C) Compound **3i** inhibited the transcription of PKM2-regulated glycolytic genes GLUT1, LDH and CCND1. HCT116 cells were treated with 20 μM compound **3i** for 8 h and qPCR was performed.

Table 2 *In vitro* inhibitory activity (IC_{50}) of **3i** and shikonin on different PKM2 isoforms

	PKM2 (μM)	PKM1 (μM)	PKL (μM)	IC_{50}(PKM1)/IC_{50}(PKM2)	IC_{50}(PKL)/IC_{50}(PKM2)
3i	0.88 ± 0.37	5.07 ± 0.13	2.90 ± 0.64	5.8	3.3
Shikonin	8.82 ± 2.62	12.96 ± 3.37	39.25 ± 6.53	1.5	4.5

various concentrations of test compounds for 48 h. Cell viability was assessed with the MTS assay (Promega) according to the manufacturer's instructions.

2.4 Measurement of ATP

HCT116 cells were seeded into 6-well plates at a density of 5 × 10^5 cells per well. 24 h after seeding, the cells were treated with 10 μM or 20 μM compound **3i** for 6 h. ATP levels were measured using the Cell Titer-Glo Luminescent Cell Viability Assay (Promega).

2.5 PKM2 activity assay

Pyruvate kinase activity was measured with a fluorescent pyruvate kinase–lactate dehydrogenase coupled assay as previously described.[20] To evaluate PKM2 activity in cell lysates, HCT116 cells were treated with various concentrations of

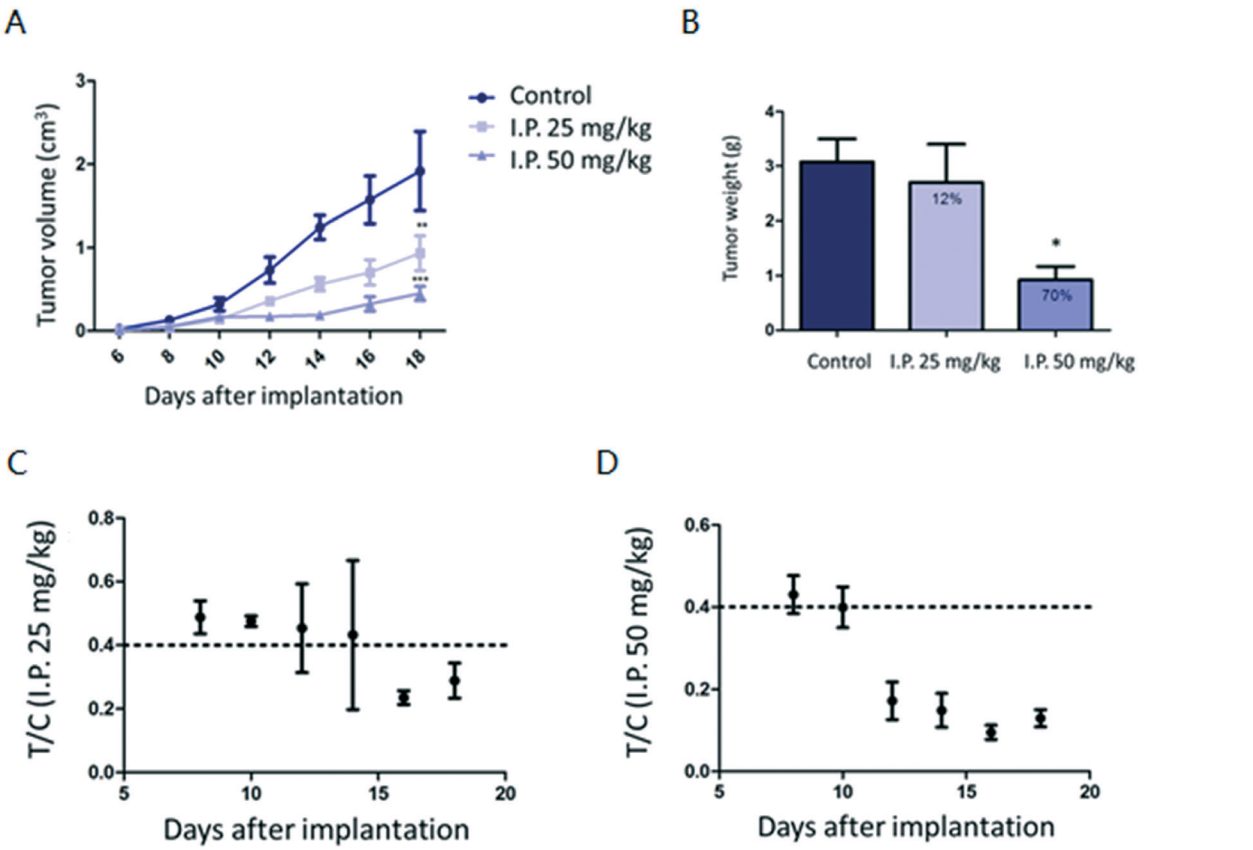

Fig. 4 Compound **3i** inhibited B16 tumor growth in a dose-dependent manner. (A) Mice were treated with 25 mg kg^{-1} or 50 mg kg^{-1} compound **3i** or vehicle. Tumor volume was measured once every two days. (B) The weight of individual tumors was measured. (C and D) The T/C values of the 25 mg kg^{-1} and 50 mg kg^{-1} treatment groups at selected time points.

compound **3i** for 8 h and lysed in NP40 lysis buffer immediately before measuring the pyruvate kinase activity as described previously.[21]

2.6 Quantitative real-time PCR (RT-qPCR)

HCT116 cells were seeded into 6-well plates at a density of 5 × 10^5 cells per well. 24 h after seeding, the cells were treated with 20 μM compound **3i** for 8 h. Total RNA was extracted using TRIzol (Invitrogen). cDNA synthesis was carried out using a cDNA synthesis kit (Transgene). qPCR was then carried out using a SYBR Green Master Mix (Transgene) in a Bio-rad real-time PCR machine. The PCR primer sequences used are listed in ESI† Table S1.

2.7 B16 melanoma transplantation mouse model

Female C57BL/6 mice were injected with 1 × 10^6 B16 cells subcutaneously in the armpits. Approximately 6 days later, B16 tumors appeared, and the mice were paired (N = 7) and injected with compound **3i** (25 mg kg^{-1} and 50 mg kg^{-1}) or the vehicle. Compound **3i** was dissolved in 5% (v/v) DMAC (dimethylacetamide) and added to olive oil. Intraperitoneal injection was performed in the mice. The animals were injected once every two days. Tumor volume was calculated using the following equation: $V = L(S^2)\pi/6$, where L is the longer and S is the shorter of the two tumor dimensions.

2.8 Spontaneous breast carcinoma mouse model

C57BL/6 spontaneous breast carcinoma mice[22] were paired (N = 3) and injected with compound **3i** (50 mg kg^{-1}) or the vehicle, when spontaneous tumor volumes reached 0.1 cm^3. Intraperitoneal injection was performed in the mice. The animals were injected once every two days.

All experiments were performed in compliance with the relevant laws and institutional guidelines of the Institute Research Ethics Committee of Peking University Health Science Center, and the committee had approved the experiments.

2.9 Statistical analysis

Statistical analysis was performed using GraphPad Prism 5.0. Data are presented as mean ± SD (n = 3).

3. Results and discussion

We prepared compound **3i** by the synthetic route shown in Fig. 1B. To determine the efficiency of compound **3i** as an anti-tumor agent, we assessed the *in vitro* cytotoxicity of **3i** using several different tumor cell lines derived from human

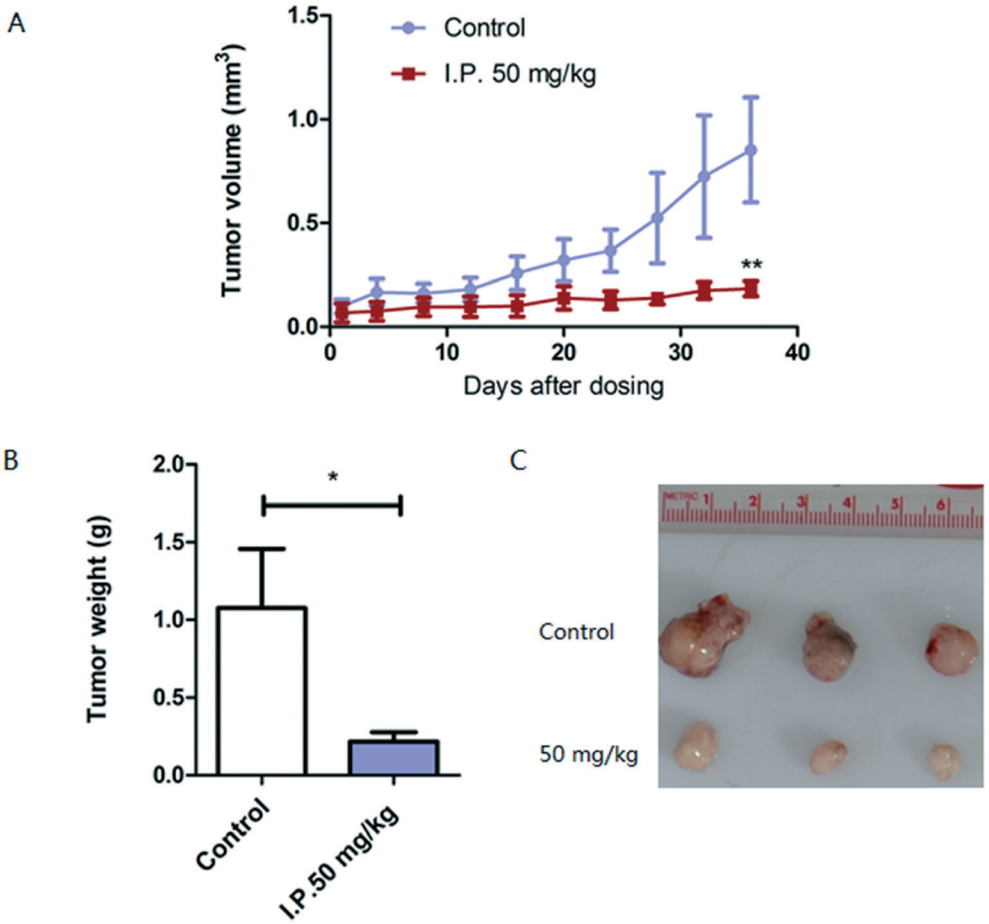

Fig. 5 Compound **3i** significantly inhibited mouse spontaneous breast tumor growth. (A) Mice were treated with compound **3i** or the vehicle. Tumor volume was measured once every four days. (B and C) Tumors were removed after sacrificing the mice. The weight of individual tumors was measured.

colon cancer (HCT116), breast cancer (MCF7), breast cancer (MDA-MB231), cervical cancer (HeLa) and lung cancer (H1299), and mouse melanoma (B16). The results are presented in Table 1. Compound **3i** reduced cancer cell viability at nanomolar concentrations with IC_{50} values against HCT116, MCF7, MDA-MB231, HeLa, H1299 and B16 cells from 50 nM to 150 nM in MTS reduction assays. In particular, compound **3i** exhibited a dose-dependent cytotoxicity (Fig. 2). To further explore the selectivity of the target compound against cancer cells, we tested its cytotoxicity in BEAS-2B cells derived from normal human bronchial epithelial cells. As seen in Table 1, compound **3i** showed higher selectivity for H1299 cancer cells than BEAS-2B normal cells, which indicated that compound **3i** probably has low toxicity to normal cells.

The direct consequence of inhibiting tumor cell metabolism is the decrease of ATP production in cells. We treated HCT116 cells with 10 μM and 20 μM compound **3i** and tested ATP production with an ATP assay kit. The results showed that compound **3i** significantly influenced the metabolic function by impairing the cellular ATP production (Fig. 3A). Compound **3i** has a similar naphthoquinone skeleton to shikonin[23] which was reported to affect the metabolism of tumor cells by inhibiting PKM2 activity, therefore, we tested the influence of compound **3i** on PKM2 activity using a fluorescence PK–LDH coupled assay according to a previously reported method.[20] Shikonin was used as the positive control. As shown in Table 2, compound **3i** (IC_{50} = 0.88 ± 0.37) displayed higher inhibitory activity than shikonin (IC_{50} = 8.82 ± 2.62). Moreover, compound **3i** showed inhibition of PKM2 with lower inhibition of PKM1 and PKL. To investigate whether compound **3i** is able to inhibit PKM2 in cells, we treated cells in which PKM2 is highly expressed with 2.5 μM, 5 μM, 10 μM and 20 μM compound **3i** and assayed PKM2 activity in the corresponding cell lysates. We found that compound **3i** inhibited PKM2 activity in cells in a dose-dependent manner (Fig. 3B). In addition, there is extensive evidence that PKM2 coactivates β-catenin to induce its downstream gene CCND1 and c-Myc transcription, resulting in upregulation of GLUT1 and LDHA. We evaluated the transcription of these genes. Cells were treated with 20 μM compound **3i**, and RT-PCR showed a significant reduction of GLUT1, LDH and CCND1 (Fig. 3C). These data suggest that compound **3i** probably interferes with the energy metabolism of cancer cells by inhibiting PKM2 activity.

Based on the potent inhibitory effect of compound **3i** on tumor cells *in vitro*, we next assessed its inhibitory efficiency in mouse models. The *in vivo* anti-tumor effect of compound **3i** was first evaluated in a B16 transplantation mouse model. As shown in Fig. 4A, intraperitoneal injection of compound **3i** at 25 and 50 mg kg^{-1} every two days for a period of 12 days demonstrated significant dose-dependent inhibition of tumor growth over the course of the treatment. The mice treated with compound **3i** at 50 mg kg^{-1} showed tumors of 30% tumor weight compared to the vehicle-treated (control) group (Fig. 4B). The T/C values (relative tumor volume growth rate) of the 50 mg kg^{-1} treatment group were close to or less than 40% at each time point, which is consistent with the high efficiency of compound **3i** (Fig. 4D). In addition, compound **3i** had no significant effect on body weight over the course of this experiment, suggesting that it was well tolerated *in vivo*.

To further assess the therapeutic efficiency of this compound, we used a PTEN deletion-mediated mouse spontaneous breast tumor model.[22] Mice were divided into two groups when tumors reached a volume of 0.1 cm^3, and compound **3i** at 50 mg kg^{-1} or the vehicle was injected intraperitoneally every two days for 36 days. As shown in Fig. 5A, tumor growth was significantly suppressed over this course of treatment. The mouse tumor weight after treatment with compound **3i** was approximately 20% of that of the control (Fig. 5B and C).

4. Conclusions

Modulation of metabolism is a key characteristic of highly proliferative cancer cells which allows both rapid ATP generation and access to metabolites needed as cellular building blocks. Here, we describe a metabolic suppressor compound **3i** which is a previously unreported compound. Compound **3i** reduced cancer cell viability in a high response with IC_{50} values in nanomolar concentrations and suppressed ATP production in cancer cells. Meanwhile, compound **3i** inhibited a rate-limiting enzyme PKM2 in the glycolytic pathway. However, the cytotoxicity of compound **3i** was much higher than the PKM2 inhibitory activity, which suggested that compound **3i** had other mechanisms to influence tumor cell metabolism and suppress cell proliferation. The 1,4-naphthoquinone moiety of compound **3i** has been reported to influence other proteins, such as DT-diaphorase[24] and the P2X7 receptor,[25] which may lead to the poor activity relationship at the enzyme and cellular levels. However, there is no doubt that compound **3i** targets PKM2 and affects tumor cell metabolism. In future studies, we will focus on investigating other mechanisms of compound **3i**.

In this study, we also found that compound **3i** significantly inhibited PTEN loss-mediated mouse spontaneous breast tumor growth. Previous studies have indicated that PTEN-negative human hepatocellular carcinoma cell lines show upregulation of PKM2 expression, which is advantageous for cell proliferation and anchorage-independent growth.[26] This probably accounts for the fact that compound **3i** is very sensitive to PTEN loss in the spontaneous tumor model. The mechanism will be investigated in our further work. In addition, we will also continue the optimization of the structure of 2,3-didithiocarbamate-substituted naphthoquinones and prepare suitable formulation for identifying new compounds with better physico-chemical properties and higher efficiency.

Conflicts of interest

The authors declare no competing interest.

Acknowledgements

This study was supported by the National Natural Science Foundation of China (Key grants #81430056, #81372491 and #81402777) and the China Postdoctoral Science Foundation (#2014M560026 and #2015T80028).

References

1 W. Yang and Z. Lu, *Cancer Lett.*, 2013, **339**, 153–158.
2 A. T. Ooi and B. N. Gomperts, *Clin. Cancer Res.*, 2015, **21**, 2440–2444.
3 J. Penkert, T. Ripperger, M. Schieck, B. Schlegelberger, D. Steinemann and T. Illig, *Oncotarget*, 2016, **7**, 67626–67649.
4 O. Warburg, *Science*, 1956, **123**, 309–314.
5 Y. Zhao, E. B. Butler and M. Tan, *Cell Death Dis.*, 2013, **4**, e532.
6 N. D. Amoedo, E. Obre and R. Rossignol, *Biochim. Biophys. Acta*, 2017, **1858**, 674–685.
7 N. E. Scharping and G. M. Delgoffe, *Vaccines*, 2016, **4**, 46.
8 N. Wong, J. De Melo and D. Tang, *Int. J. Cell Biol.*, 2013, **2013**, 242513.
9 V. Gupta and R. N. Bamezai, *Protein Sci.*, 2010, **19**, 2031–2044.
10 W. Luo and G. L. Semenza, *Trends Endocrinol. Metab.*, 2012, **23**, 560–566.
11 T. Noguchi, H. Inoue and T. Tanaka, *J. Biol. Chem.*, 1986, **261**, 13807–13812.
12 W. Yang and Z. Lu, *J. Cell Sci.*, 2015, **128**, 1655–1660.
13 H. R. Christofk, M. G. Vander Heiden, M. H. Harris, A. Ramanathan, R. E. Gerszten, R. Wei, M. D. Fleming, S. L. Schreiber and L. C. Cantley, *Nature*, 2008, **452**, 230–233.
14 W. Yang, Y. Xia, H. Ji, Y. Zheng, J. Liang, W. Huang, X. Gao, K. Aldape and Z. Lu, *Nature*, 2011, **480**, 118–122.
15 T. L. Dayton, T. Jacks and M. G. Vander Heiden, *EMBO Rep.*, 2016, **17**, 1721–1730.
16 X. Gao, H. Wang, J. J. Yang, X. Liu and Z. R. Liu, *Mol. Cell*, 2012, **45**, 598–609.
17 X. Gao, H. Wang, J. J. Yang, J. Chen, J. Jie, L. Li, Y. Zhang and Z. R. Liu, *J. Biol. Chem.*, 2013, **288**, 15971–15979.
18 X. Ning, H. Qi, R. Li, Y. Li, Y. Jin, M. A. McNutt, J. Liu and Y. Yin, *Eur. J. Med. Chem.*, 2017, **138**, 343–352.

19 X. Ning, H. Qi, R. Li, Y. Jin, M. A. McNutt and Y. Yin, *J. Enzyme Inhib. Med. Chem.*, 2018, **33**, 126–129.
20 M. G. Vander Heiden, H. R. Christofk, E. Schuman, A. O. Subtelny, H. Sharfi, E. E. Harlow, J. Xian and L. C. Cantley, *Biochem. Pharmacol.*, 2010, **79**, 1118–1124.
21 H. R. Christofk, M. G. Vander Heiden, N. Wu, J. M. Asara and L. C. Cantley, *Nature*, 2008, **452**, 181–186.
22 A. Di Cristofano, B. Pesce, C. Cordon-Cardo and P. P. Pandolfi, *Nat. Genet.*, 1998, **19**, 348–355.
23 J. Chen, J. Xie, Z. Jiang, B. Wang, Y. Wang and X. Hu, *Oncogene*, 2011, **30**, 4297–4306.
24 C. Flader, J. Liu and R. F. Borch, *J. Med. Chem.*, 2000, **43**, 3157–3167.
25 R. X. Faria, F. H. Oliveira, J. P. Salles, A. S. Oliveira, N. L. von Ranke, M. L. Bello, C. R. Rodrigues, H. C. Castro, A. R. Louvis, D. L. Martins and V. F. Ferreira, *Eur. J. Med. Chem.*, 2018, **143**, 1361–1372.
26 I. Nemazanyy, C. Espeillac, M. Pende and G. Panasyuk, *Biochem. Soc. Trans.*, 2013, **41**, 917–922.

